Meso/micro scale milling for micro-manufacturing

A. Dhanorker and T. Özel*

Department of Industrial and Systems Engineering,
Rutgers University, Piscataway, NJ 08854-8018, USA
E-mail: atuld@eden.rutgers.edu
E-mail: ozel@rci.rutgers.edu
*Corresponding author

Abstract: Meso/micro scale milling is a direct operation to manufacture miniature parts. In this paper, experimental and modelling studies on meso/micro-milling of AL 2024-T6 aluminum and AISI 4340 steel are presented. Experiments include dynamic force measurements. The finite element modelling of meso/micro-milling is also conducted to predict chip formation and temperature fields. Size effects and minimum chip thickness related to edge radius and chip load on the workpiece deformations are also investigated. Process simulations are validated for force predictions.

Keywords: micro-milling; finite element modelling; size effect; minimum chip thickness.

Reference to this paper should be made as follows: Dhanorker, A. and Özel, T. (2008) 'Meso/micro scale milling for micro-manufacturing', *Int. J. Mechatronics and Manufacturing Systems*, Vol. 1, No. 1, pp.23–42.

Biographical notes: A. Dhanorker received his MS in Industrial and Systems Engineering from Rutgers University, USA in 2007. His research interest includes analytical and computational modelling of meso/micro milling processes.

T. Özel received his PhD in Mechanical Engineering from The Ohio State University, USA in 1998. He is an Assistant Professor of Industrial and Systems Engineering at Rutgers University. His research interest includes modelling of machining processes, automation and process control, optimisation of processes and systems, and micro/nano manufacturing. He has over ten years of experience about manufacturing research. He has been reviewer, organiser, guest editor and editorial board member for several journals and conferences. He has published over 50 refereed papers.

1 Introduction

The demand for miniaturised meso-(1–10 mm)/micro-(1–1000 μm) devices with high aspect ratios and superior surfaces has been rapidly increasing in aerospace, automotive, biomedical, optical, military and micro-electronics packaging industries (Alting et al., 2003; de Chiffre et al., 2003; Madou, 1997). There is a growing need for fast, direct, and mass manufacturing of miniaturised functional products from metals, polymers, composites, and ceramics.

Mechanical micromachining, scaled down versions of turning, milling and drilling, as a cluster of micro-manufacturing processes is rapidly gaining momentum because of its viability to directly produce miniature 3-D functional parts (Dornfeld et al., 2006; Masuzawa and Tonshoff, 1997; Friedrich and Vasile, 1996; Schaller et al., 1996; Vasile et al., 1999). Among those, micro-milling process is not only fast to fabricate 3-D features but also cost efficient as compared to other micro-manufacturing processes. Parts with 3-D geometry are directly machined one at a time not requiring batch set-up. Micro-milling can achieve good accuracy, low surface roughness, and can provide high Material Removal Rates (MRR) with feature sizes as small as 5–10 μm particularly with recently developed miniature machine tools (Vogler et al., 2002). Micro end mills with diameters down to 25 μm, mostly made of tungsten-carbide on cobalt matrix (WC-Co), are available on the market. Such micro end mills are utilised in direct fabrication of micro-molds/dies from tool steels for injection molding and micro-forming applications (Weule et al., 2001; Uhlmann and Schauer, 2005; Schmidt et al., 2002; Schmidt and Tritschler, 2004). Improving productivity for micro-milling requires use of high material removal rates on a variety of materials. However, there are still issues associated with the dimensional accuracy, quality of the surfaces generated and sudden tool failure.

Increasing popularity of micro-manufacturing has sparked the interest of researchers to study the micro-milling to improve the productivity and also to understand how it differs from conventional milling (Bao and Tansel, 2000a, 2000b, 2000c). The fundamental difference between micro-milling and conventional milling arises due to scale of the operation, while they are kinematically the same. However, the ratio of feed per tooth to radius of the cutter is much greater in micro-milling than conventional milling, which often leads to an error in predicting cutting forces (Bao and Tansel, 2000a). The runout of the tool tip even within microns greatly affects the accuracy of micro-milling as opposed to the conventional milling (Bao and Tansel, 2000b). Micro-milling is associated with sudden tool failure due to its highly unpredictable cutting action (Bao and Tansel, 2000c). The chip formation in the micro-milling depends upon a minimum chip thickness (Ikawa et al., 1992) and hence the chip is not always formed whenever tool and workpiece is engaged as opposed to conventional milling (Kim et al., 2002, 2004). The tool deflection in the micro-milling greatly affects the chip formation and accuracy of the desired surface as compared to conventional milling (Dow et al., 2004). The tool edge radius (typically between 1–5 μm) and its uniformity along the cutting edge is highly important as the chip thickness becomes a comparable in size to the cutting edge radius (Lucca, 1993; Melkote and Endres and Seo, 1998). Since the chip load is small compared to the cutting edge radius, the size effect and ploughing forces become significant on both surface and force generation in micro-milling (Vogler et al., 2004a, 2004b). Micro-milling may result in surface generation with burrs and increased roughness due to the ploughing-dominated cutting and side flow of the deformed material when the cutting edge becomes worn and blunter (Lee and Dornfeld, 2002).

1.1 Size effect and minimum chip thickness

The current manufacturing method cannot fabricate end mills, mostly made of WC-Co, with sharp edges due to limitation of structural strength of the tool at the edge. Widely available micro tools have edge radius ranging from 1 μm to 5 μm. As the tool diameter decreases, the rigidity of the tool also decreases which leads to tool deflections

under heavy chip load and sudden breakage of tool. This limits the chip load, especially in micro-milling, to a few microns per tooth. With the small feed rates the well known size effect, originally discovered in ultra precision diamond cutting (Ikawa et al., 1992), becomes prominent in micro-milling. Specific cutting forces also depend mostly on the ratio of the uncut chip thickness to the tool edge radius.

The tool edge radius and small feed per tooth makes the phenomenon of minimum chip thickness highly predominant in the micro-milling. A minimum chip thickness is observed where tool engagement with workpiece results in chip formation. In full-immersion micro-milling uncut chip thickness of $t_u(\phi)$ varies from zero to feed per tooth of f_z as shown in Figure 1. Hence the minimum chip thickness for micro-milling (t_{c_min}) can be defined as formation of chip when the uncut chip thickness becomes greater than a minimum chip thickness ($t_u > t_{c\_min}$) at a certain rotation angle of ϕ. Unlike precision diamond turning where diamond tools are up-sharp with nano-metric edge radius, the minimum chip thickness in micro-milling is greatly affected by the radius of the cutting edge (r_e) which is usually greater than 1 µm (see Figure 2). The chip is not formed and mostly elastic deformations are induced to the workpiece until tool reaches to a certain rotation angle where a minimum uncut chip thickness develops. A smaller edge radius causes early formation of minimum chip thickness whereas a larger edge radius will result in ploughing of the workpiece. Kim et al. (2004) experimentally determined that minimum chip thickness depends upon the ratio of uncut chip thickness to the cutting edge radius which was claimed between 10% and 25% for the ductile metals. Liu et al. (2006) calculated the minimum chip thickness and utilised a ratio ($\lambda = t_{c\_min}/r_e$) to describe as function of edge radius. In that study, minimum chip thickness to tool edge radius ratio was found about 35–40% for micro-milling of AL6082-T6 aluminum and 20–30% for AISI 1018 steel at a wide range of cutting speed and edge radius.

Figure 1 Chip thickness and planar forces during micro-milling process

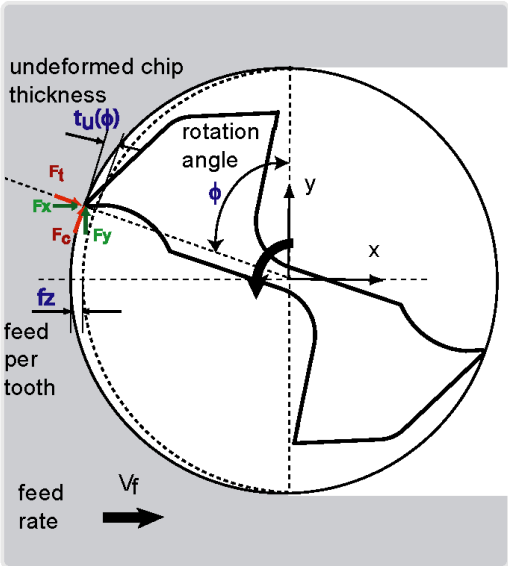

Figure 2 The minimum chip thickness phenomenon in micro-milling: (a) uncut chip load less than a minimum required and (b) uncut chip load sufficient to form a chip

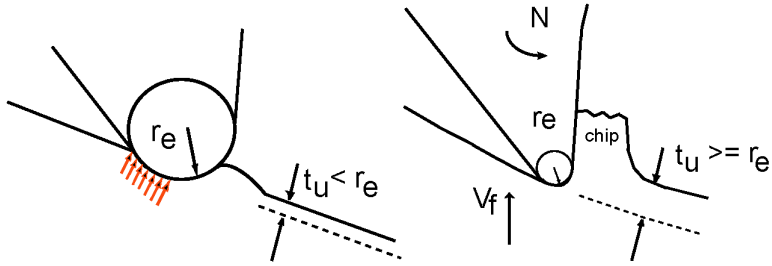

(a) (b)

2 Experimental procedure

2.1 Meso scale milling experiments

Meso scale milling experiments using flat end cutters are conducted by taking slot cuts at a constant axial depth of cut and spindle speed in machining of AL 2024-T6 workpiece in a 3-axis vertical CNC milling machine. Two different tool diameters for 2-flute carbide end mills are used with varying feed per tooth to investigate the effect of feed rate on the cutting forces generated. The cutting forces were acquired using a piezo-electric dynamometer and charge amplifier (Kistler, models 9265C2 and 5010). There global axis forces (x,y, and z directional forces) have been recorded at 50 kHz with a PC-based data acquisition system. A summary of the experimental conditions is given in Table 1.

Forces acting on the tool in full-immersion (slot milling) conditions are shown in Figure 3. The forces in the feed and normal directions are F_x and F_y, respectively. The force components along the radial and orthogonal to the radial directions are thrust (F_t) and cutting (F_c) forces respectively.

Figure 3 (a) Meso end mill (D = 1.5875 mm); (b) micro end mill (D = 0.635 mm) and (c) slot milling operation

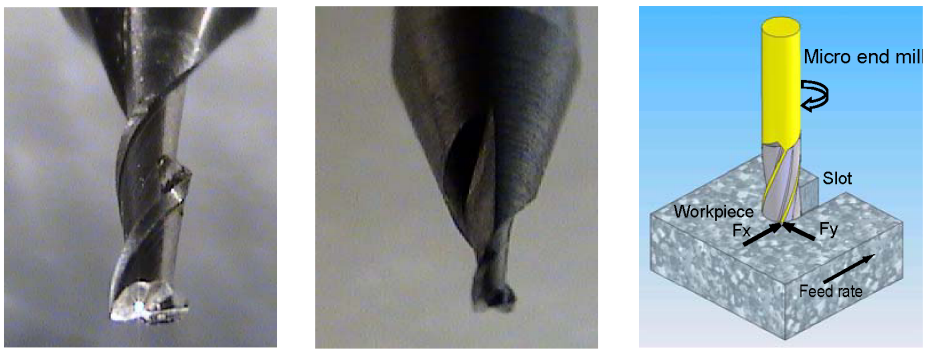

(a) (b) (c)

Table 1 Meso-end milling experiments

Material	*AL 2024-T6 Aluminum*
Tool	2- Flute WC-Co End Mill with 30^0 helix angle
Tool diameter (mm)	1.5875, 3.175
Axial depth of cut (mm)	1.27
Spindle speed (rpm)	6000
Cutting speed (m/min)	22.62, 59.85
Feed per tooth (µm)	0.265, 0.53, 1, 2, 4

Size effect and minimum chip thickness were investigated in these experiments by varying feed rate to obtain a feed per tooth from 4 µm to 0.265 µm. Tool cutting edge radius for 1.5875 mm diameter tool is found about 10 µm and for 3.175 mm tool is about 20 µm as suggested by the manufacturer. Measured feed (F_x) and normal forces (F_y) in various feed rates in meso-end milling with 1.5875 mm diameter end mill are given in Figure 4. It is seen that the forces increase with the increase in the feed rate. However, the specific cutting forces are increasing with decreasing feed rate as shown in Figure 5. It should be noted that the minimum chip thickness is observed at around a feed rate of 0.53 µm/tooth in this case. For feed rates of 0.265 and 0.53 µm/tooth, the specific forces are significantly higher, indicating that the ploughing-dominated end milling takes place at those cutting conditions, whereas, shearing-dominated end milling is seen in the other feed rates. Measured feed (F_x) and normal (F_y) forces in various feed rates for the 3.175 mm diameter end mill are also given in Figure 6. The variation in the measured forces are much greater in meso end milling with 1.5875 mm diameter end mill, when compared to the measured forces in meso end milling with 3.175 mm diameter end mill. This can be explained that as the diameter of the end mill is chosen smaller the flexural stiffness gets lower, hence the force variations increased due to the reduced stiffness of the cutter and increased elastic deformations.

Figure 4 Measured feed and normal forces in various feed rates in meso-end milling (D = 1.5875 mm): (a) feed force and (b) normal force

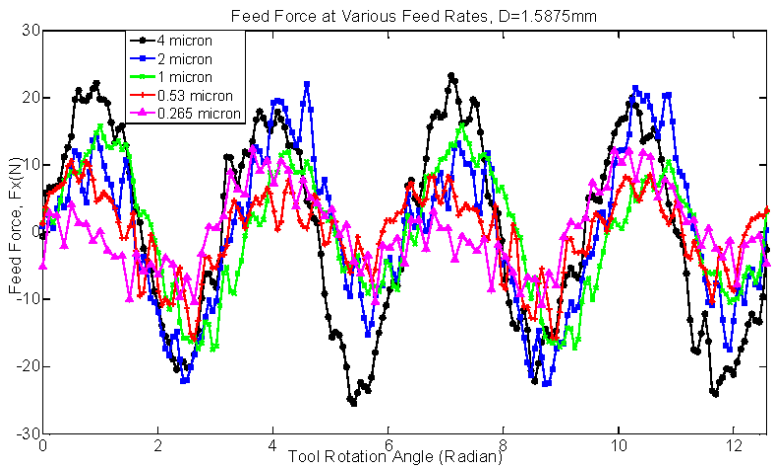

(a)

Figure 4 Measured feed and normal forces in various feed rates in meso-end milling (D = 1.5875 mm): (a) feed force and (b) normal force (continued)

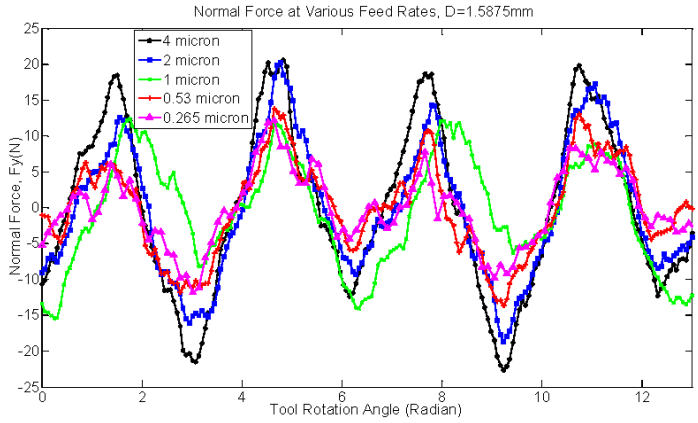

(b)

Figure 5 Specific feed and normal forces in various feed rates in meso-end milling (D = 1.5875 mm): (a) specific feed force and (b) specific normal force

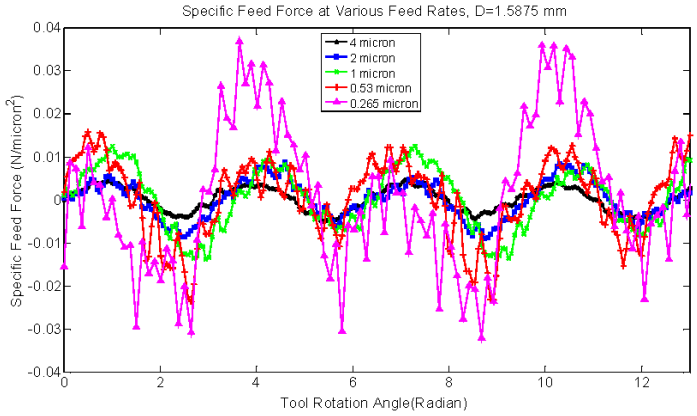

(a)

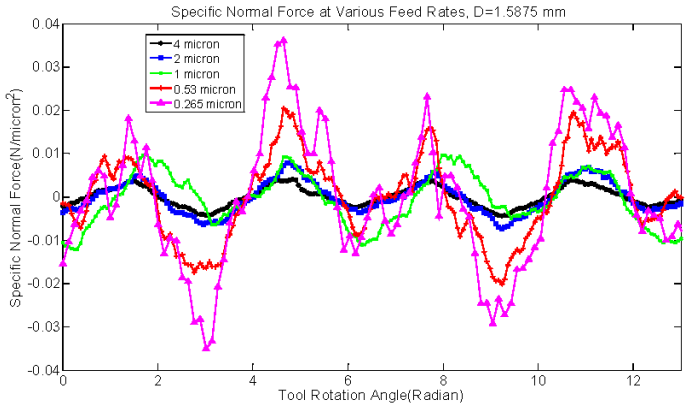

(b)

Figure 6 Measured feed and normal forces in various feed rates in meso-end milling (D = 3.175 mm): (a) feed force and (b) normal force

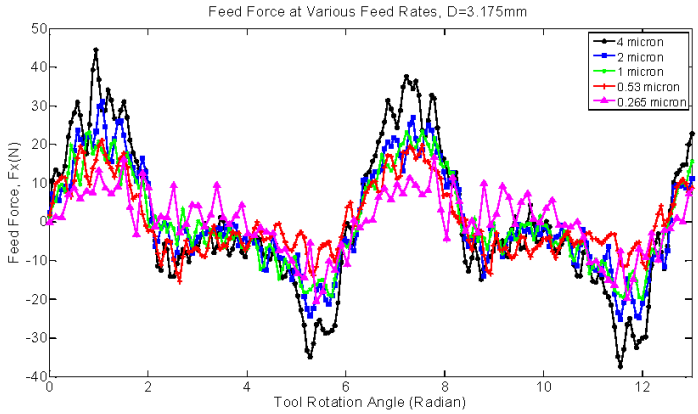

(a)

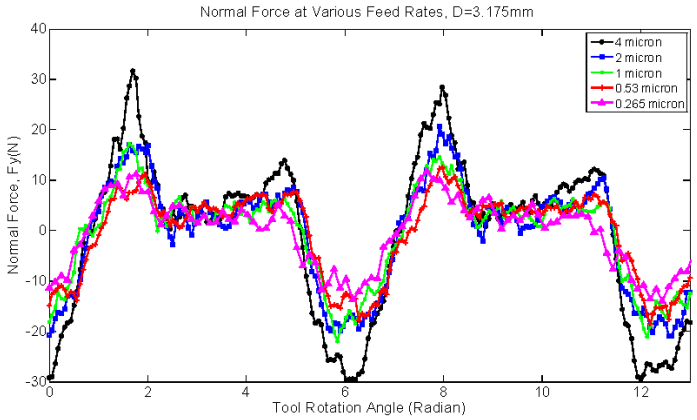

(b)

2.2 Micro scale milling experiments

Micro-milling experiments using flat bottom micro end mils are also conducted by taking slot cuts (full immersion) at a constant axial depth of cut and spindle speed for AL2024-T6 aluminum and AISI 4340 steel. The summary of the experimental conditions is given in Table 2. A micro end mill with 0.635 mm diameter with 2-flutes is used with varying feed per tooth to investigate the effect of feed rate on the cutting forces generated. The microscopic picture of the WC-Co micro end mill is shown in Figure 3(b). The cutting forces were acquired using a piezo-electric dynamometer and charge amplifier (Kistler, models 9257B and 5010) with an estimated uncertainty about ±0.2 N. The (x, y and z) global axis forces have been recorded at 2667, 4000 and 5333 Hz for the spindle speed of 40000, 60000, and 80000 rpm respectively with a PC-based data acquisition system and Kistler DynoWare software. The force signals at each channel of the dynamometer are sampled with twice the tooth passing frequency; hence four samples were collected per rotation.

Table 2 Micro-end milling experiment parameters

Material	*AL 2024-T6 aluminum and AISI 4340 steel*
Tool	2- Flute Carbide End Mill with 30^0 helix angle
Tool diameter (mm)	0.635
Axial depth of cut (mm)	0.127
Spindle speed (rpm)	40000, 60000, 80000
Cutting speed (m/min)	79.8, 119.7, 169.65
Feed per tooth (μm)	1.27, 2.54, 5.08

Figure 7 Measured feed and normal forces (N/mm) at 2.54 μm feed per tooth feed rate and at various rpm spindle speed in micro-end milling of AL2024-T6: (a) feed force and (b) normal force

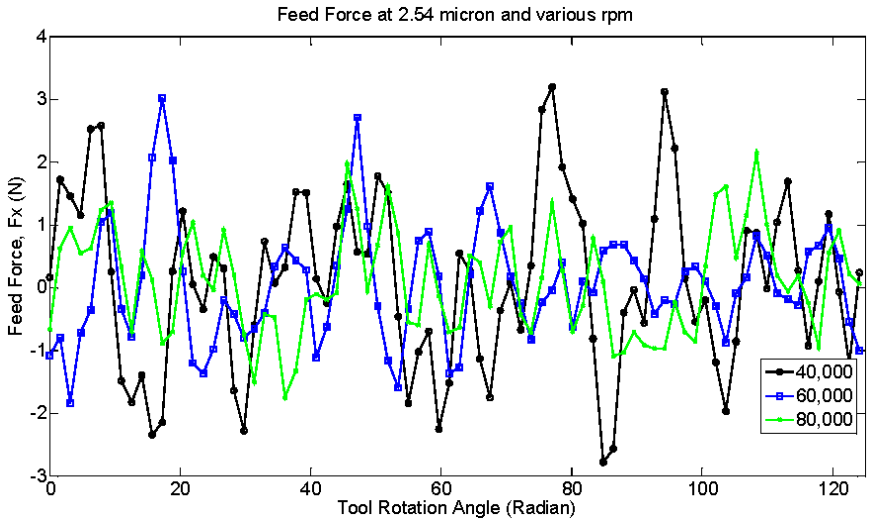

(a)

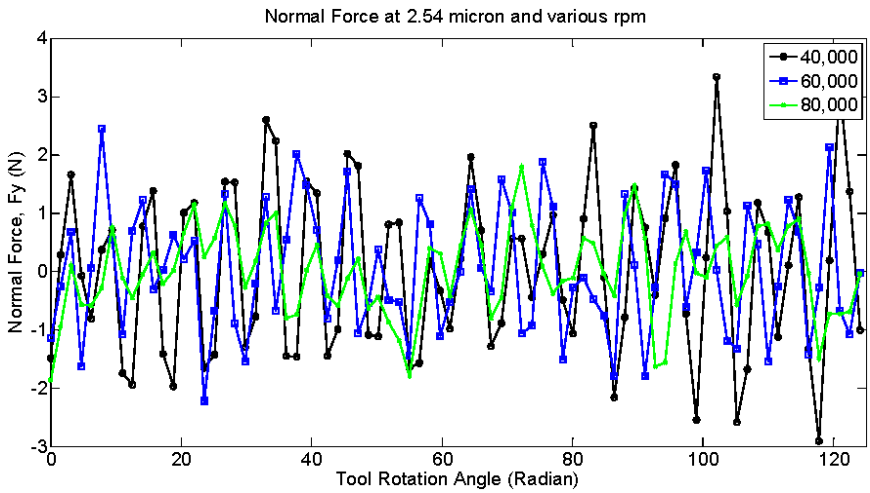

(b)

Experimentally measured feed (Fx) and normal forces (Fy) for a constant feed rate of 2.54 µm for three different spindle speeds (40 krpm, 60 krpm, 80 krpm) in micro-milling of AL2024-T6 aluminum are given in Figure 7. Experimentally measured feed and normal forces at 40,000 rpm spindle speed at various feed per tooth (1.27 µm, 2.54 µm, 5.08 µm) in micro-end milling of AISI 4340 steel are shown in Figure 8. Measured forces showed large fluctuations due to process dynamics and continuous shift between ploughing and shearing dominated cutting during micro-milling. There is also the effect of the low sampling rate on the fluctuation of the measured forces. Since there are only four samples collected in one rotation, detailed force generation within a full rotation could not be observed. High bandwidth and high sampling frequency force measurement capability is required for better understanding of the force generation in micro-milling.

Figure 8 Measured feed and normal forces (N/mm) at 40,000 rpm spindle speed and at various feed per tooth in micro-end milling of AISI 4340 steel: (a) feed force and (b) normal force

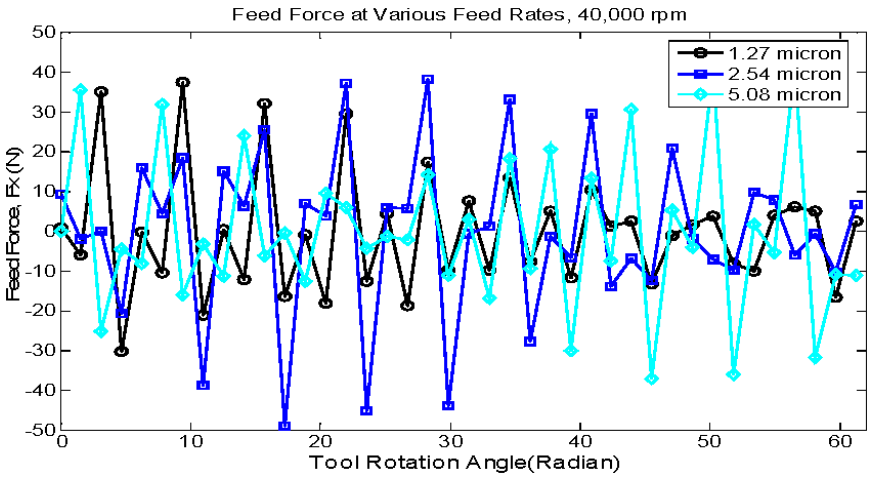

(a)

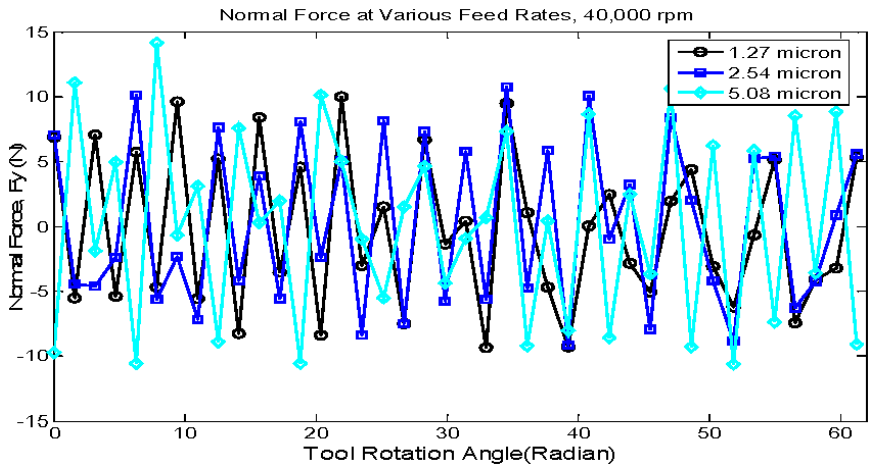

(b)

3 Influence of edge radius on minimum chip thickness

The influence of edge radius on minimum chip thickness for micro-milling of AL2024-T6 and AISI 4340 steel is investigated by utilising an analytical model developed by Liu et al. (2006). In their analytical model, workpiece material model and a slip-line field analysis are utilised in estimating the minimum chip thickness for a given tool edge radius, feed rate and surface cutting speed. This analytical model accounts for strain hardening, thermal softening and elastic recovery effects of work material with Johnson-Cook constitutive model under high strain, strain-rate and temperate conditions.

The Johnson-Cook model (Johnson and Cook, 1983) describes the flow stress of a material with the product of strain, strain rate and temperature effects that are individually determined as given in equation (1). In the Johnson-Cook (J-C) model, the constant A is the initial yield strength of the material at room temperature and a strain rate of $1/s$ and ε represents the plastic equivalent strain. The strain rate ε is normalised with a reference strain rate of ε_0. Temperature term in the J-C model reduces the flow stress to zero at the melting temperature of the work material, leaving the constitutive model with no temperature effect.

$$\bar{\sigma} = [A + B(\bar{\varepsilon})^n]\left[1 + C\ln\left(\frac{\dot{\bar{\varepsilon}}}{\dot{\bar{\varepsilon}}_0}\right)\right]\left[1 - \left(\frac{T - T_{room}}{T_{melt} - T_{room}}\right)^m\right]. \quad (1)$$

The Johnson-Cook work material model parameters for AISI 4340 steel and AL 2024-T6 aluminum are given in Table 3. Thermo mechanical properties for work and tool materials are also given in Table 4.

Table 3 Johnson-Cook material model constants

Material	*A* (MPa)	*B* (MPa)	*n*	*C*	*m*	T_{melt} (ºC)
AISI 4340	792	510	0.26	0.0140	1.03	1520
AL 2024-T6	369	684	0.73	0.0083	1.70	502

Table 4 Thermo mechanical properties of work and tool materials

	AISI 4340	*AL 2024-T6*	*WC-Co*
Density (g/cm^3)	7.85	2.78	15.7
Modulus of elasticity (GPa)	205	73.1	650
Poisson's ratio	0.29	0.33	0.25
Specific heat capacity (J/g-ºC)	0.475	0.875	0.26
Thermal conductivity (W/m-K)	44.5	121	28.4
Thermal expansion (µm/m-ºC)	12.3	23.2	5.2

By using the analytical model developed by Liu et al. (2006), the minimum chip thickness to edge radius ratio for the work material of AISI 4340 steel is estimated to be between 30% and 36% for the range of edge radius (1–5 µm) and the cutting speed (120–360 m/min) as shown in Figure 9. For the work material of AL 2024-T6 aluminum, the minimum chip thickness to edge radius ratio is estimated to be between 42% and 45%

for the range of edge radius (1–5 μm) and the cutting speed (120–360 m/min) as shown in Figure 10. A particular cutter rotation angle where the minimum chip thickness is achieved and chip begins to form is denoted as Chip Formation Angle (CFA) as illustrated in Figure 2(b). Chip formation angle in relation to the uncut chip thickness, $t_u(\phi)$, can be calculated by using the analytical model developed by Liu et al. (2006).Variation of chip formation angle with respect to tool edge radius and workpiece feed rate is computed for micro-milling of AISI 4340 steel and AL2024-T6 aluminum as shown in Figures 11 and 12.

Figure 9 Predicted minimum chip thickness in micro-milling of AISI 4340 steel: (a) varying edge radius and (b) varying cutting speed

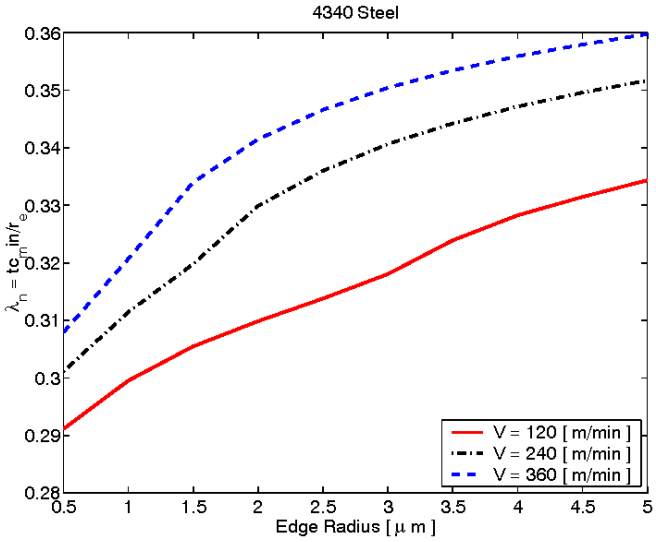

(a)

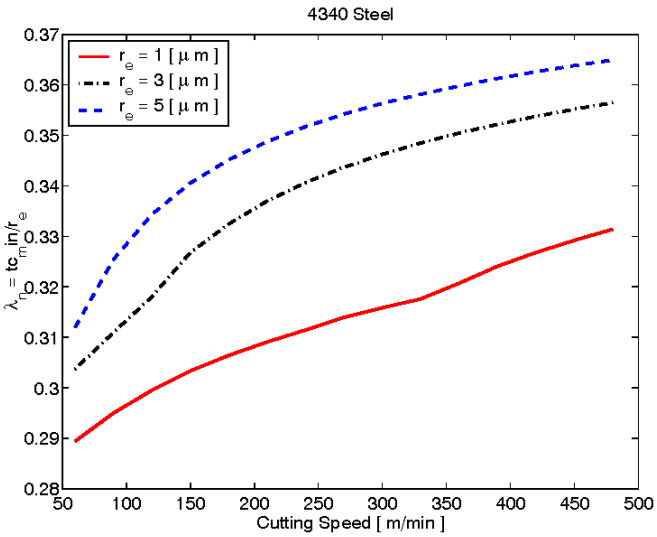

(b)

Figure 10 Predicted minimum chip thickness in micro-milling of AL 2024-T6 aluminum: (a) varying edge radius and (b) varying cutting speed

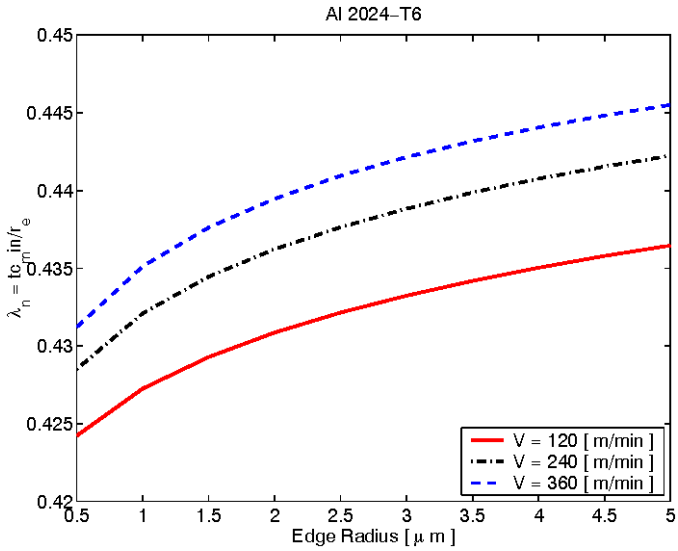

(a)

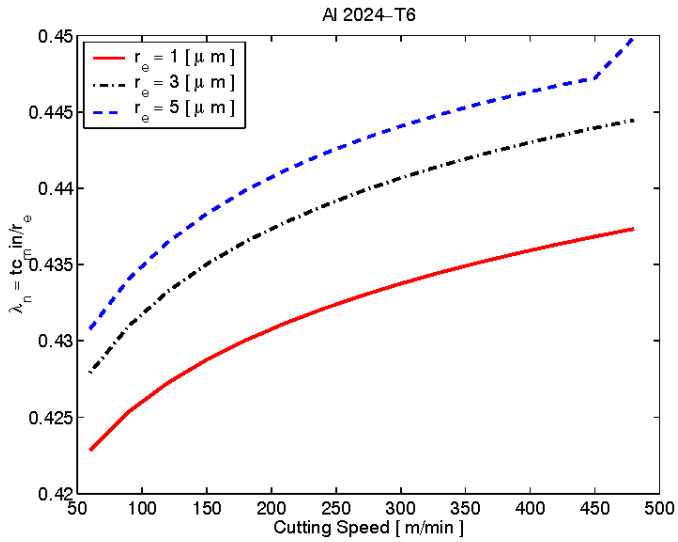

(b)

For micro-milling of AISI 4340 steel and AL2024-T6 aluminum, Figure 11(a) and 12(a) depict the relationship in the plane of CFA/r_e with three levels of feed per tooth where as Figures 11(b) and 12(b) show the relationship in the plane of CFA/f_t with three level of edge radius respectively. CFA is found to be larger in micro-milling of AL2024-T6 aluminum compared to micro-milling of AISI 4340 steel. This may be due to higher modulus of elasticity of AISI 4340 steel, where elastic tool deformations are smaller. Hence, plastic flow begins at a lower uncut chip thickness.

Figure 11 (a) Chip formation angle vs. tool edge radius and (b) chip formation angle vs. feed per tooth (AISI 4340 Steel)

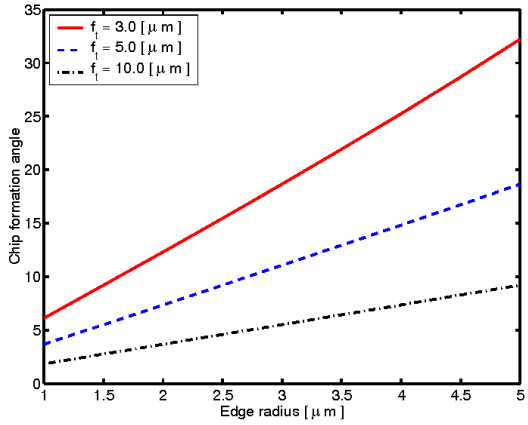

(a)

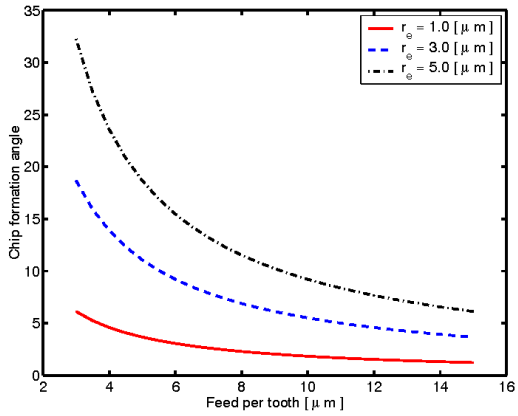

(b)

Figure 12 (a) Chip formation angle vs. tool edge radius and (b) chip formation angle vs. feed per tooth (AL 2024-T6 aluminum)

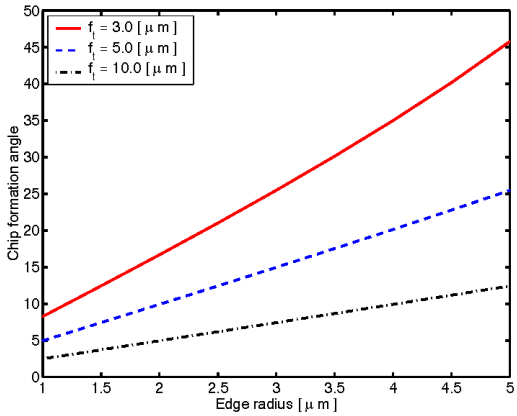

(a)

Figure 12 (a) Chip formation angle vs. tool edge radius and (b) chip formation angle vs. feed per tooth (AL 2024-T6 aluminum) (continued)

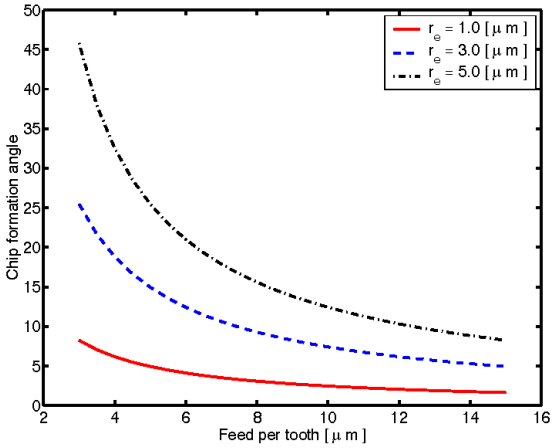

(b)

4 Finite element modelling

Cutting process can be considered as a deformation process that is highly concentrated in a small zone. Thus, chip formation in milling process can be simulated using Finite Element Method (FEM) (Özel and Altan, 2000). The main advantage of using such an approach is to be able to predict chip flow, cutting forces, and especially a distribution of tool temperatures and stresses for various cutting conditions.

In this paper, FEM simulation of meso/micro end milling process is also presented. Commercially available software, DEFORM-2D, was used for FEM simulations. Johnson-Cook workpiece material model is used for rigid-plastic deformation analysis for AL2024-T6 aluminum and AISI 4340 steel workpiece (Table 3). FEM simulations are conducted for the cutting condition of 1.5875 mm and 3.175 mm end mill diameter, 2.54 μm feed per tooth, and 6000 rev/min spindle speed in meso scale milling of AL 2024-T6. A constant friction factor of 0.65 at the chip-tool contact is used. Tool edge radius of 10 μm is used as suggested by manufacturer.

One of the preliminary tasks of this study was to investigate the tool tip path. The real motion of the tool is trochoidal. It is said to be possible to simulate the motion path as circular, when the feed is small (Martellotti, 1945). In this model the uncut chip geometry is derived by intersecting two circles whose centres are at a distance equal to the feed per tooth from each other. The uncut chip geometry in the two circles model and the tool trochoidal path are given in Figure 13. If the chip thickness is the distance between point A and B as shown in Figure 13(a), the distance of the actual center of rotation becomes equal to the feed per tooth increased by the difference of phase between the angles β and α, as given in equation (2).

$$\overline{O'O''} = f_z + (\beta - \alpha) \cdot \frac{V_f}{\varpi} \tag{2}$$

where ϖ is the spindle speed and f_z is the feed rate. Hence, computed trochoidal path is utilised in designing workpiece geometry in the FEM model for the milling process.

Figure 13 Calculation of the chip thickness: (a) two circles approach and (b) trochoidal path approach

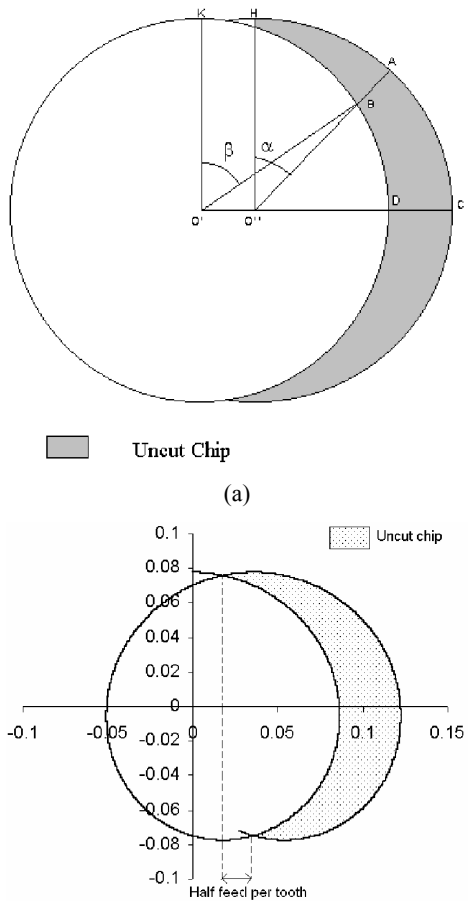

Temperature distribution for the fully-grown chip in meso-milling with end mill diameter of $D = 3.175$ mm is observed at around 90°C of tool immersion angle as shown in Figure 14. Maximum temperature rise in the cutting zone was found around 334°C. It can be claimed that heat generated due to cutting during meso end milling is not significant, compared to conventional end milling process, since chip load is much smaller. It should also be noted that FEM model assumes plain strain deformations and steady chip load, which may be inconsistent in real end milling conditions due to cutter runout.

The normal and feed forces are also predicted with the FEM simulations for the end milling diameter of 1.5875 mm as shown in Figure 15. Model validation is performed with comparison of forces predicted and measured. A comparison of the predicted and measured forces for the half rotation of the end mill indicates reasonable agreements.

Figure 14 Predicted temperature distributions in meso end milling of AL 2024-T6 aluminum

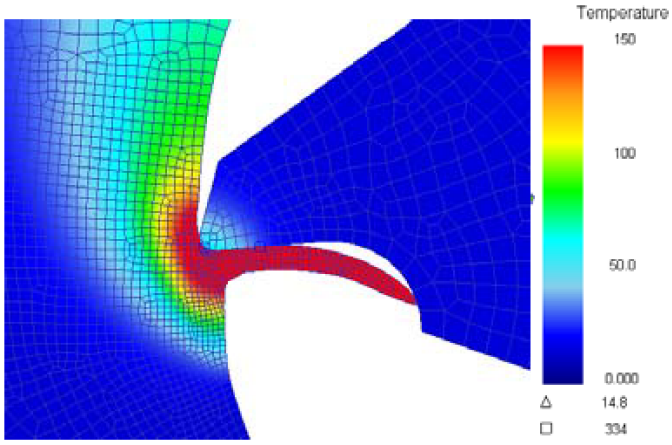

Figure 15 Comparison of predicted and measured forces in meso milling: (a) normal force and (b) feed force

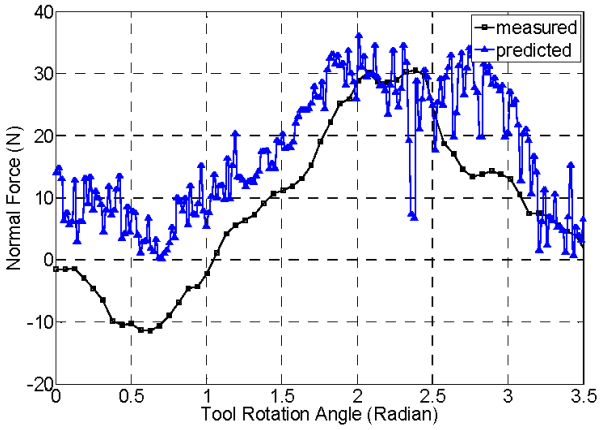

(a)

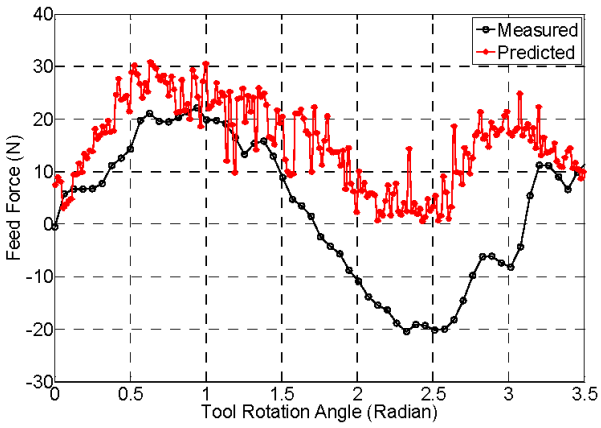

(b)

In addition, FEM simulations of the micro-milling process are also conducted. FEM models designed for micro-milling of AL2024-T6 aluminum and AISI 4340 steel are shown in Figure 16.

Johnson-Cook workpiece material model in equation (1) and its parameters (see Table 3) is used for rigid-perfectly plastic deformation analysis. FEM simulations are conducted for the cutting condition of 80 m/min surface cutting speed and 10 µm feed per tooth using the micro-end mill shown in Figure 3(b) with 0.635 mm tool diameter and 3 µm tool edge radius. A constant friction factor of 0.65 at the chip-tool-workpiece contacts is used.

Figure 16 FEM simulation of micro-milling: (a) AL2024-T6 aluminum and (b) AISI 4340 steel

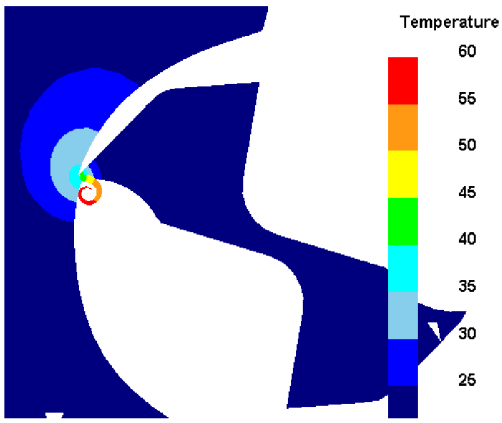

(a)

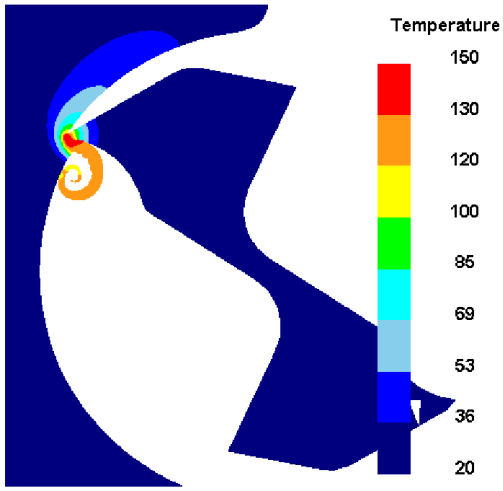

(b)

The fully developed continuous chip was simulated at a tool rotation angle of 65°C for micro-milling of AL2024-T6 aluminum as shown in Figure 16(a). A complete chip formation is observed around 53°C of tool rotation angle in micro-milling of AISI 4340 steel as shown in Figure 16(b) under the same cutting conditions.

Predicted temperature distributions are also given in Figure 17. Maximum temperatures in the cutting zone are predicted around 60°C for AL2024-T6 aluminum and around 150°C for AISI 4340 steel at the same cutting conditions. These temperatures are very low when compared to the temperatures in meso-milling conditions due to the very small chip loads.

Figure 17 Predicted temperature distributions (°C) in the cutting zone during micro-milling: (a) AL2024-T6 aluminum and (b) AISI 4340 steel

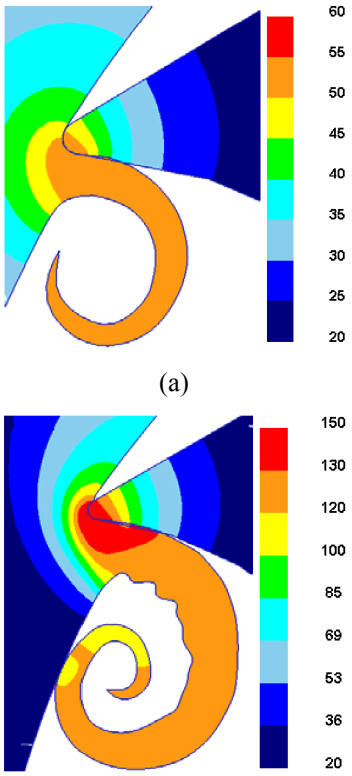

Typically tool failure is considered due to temperature-depended accelerated wear rates in high-speed milling at conventional scale. In contrast, temperature dependent wear cannot be dominant in micro-milling as evident in predicted temperature distributions in Figure 17. It is believed that highly fluctuating forces due to a continuous shift between ploughing and shearing dominated cutting modes in micro-milling are also responsible for the sudden tool failure and breakage.

5 Conclusions

This paper presents an experimental and modelling study for meso end milling of AL2024-T6 aluminum alloy. The size effect and minimum chip thickness phenomenon are also observed at very low feed rates. Large force variations are observed as the

diameter of the cutter decreases and the spindle speed increases. First, an FEM model is introduced for simulation of chip flow and predictions for forces and temperature fields in meso end milling. A comparison of predicted and measured forces for half rotation of the end mill is provided. The results are found promising to extend this FEM model to further investigate micro-end milling process.

In addition, experimental and modelling studies on micro-milling of AL 2024-T6 aluminum and AISI 4340 steel are also presented. Measured forces showed large fluctuations due to process dynamics and continuous shift between ploughing and shearing dominated cutting during micro-milling.

The minimum chip thickness to edge radius ratio is estimated to be between 42% and 45% for AL2024-T6 aluminum and between 30% and 36% for AISI 4340 steel for the given range of edge radius (1–5 μm) and the surface cutting speed (120–360 m/min). Chip formation angle and its variation with respect to micro-milling conditions are also determined.

The FEM simulations for micro-milling based on rigid-plastic deformations is also conducted to predict chip formation, forces, strain, strain-rate and temperature fields without considering process dynamics. Temperature rises due to cutting action in micro-milling are found to be negligible to cause tool wear.

Acknowledgement

The authors greatly acknowledge the assistance from Dr. Xinyu Liu in analytical predictions of minimum chip thickness and chip formation angles.

References

Alting, L., Kimura, F., Hansen, H.N. and Bissacco, G. (2003) 'Micro engineering', *Annals of the CIRP*, Vol. 52, No. 2, pp.635–657.

Bao, W.Y. and Tansel, I.N. (2000a) 'Modeling micro-end-milling operations. Part I: analytical cutting force model', *International Journal of Machine Tools and Manufacture*, Vol. 40, pp.2155–2173.

Bao, W.Y. and Tansel, I.N. (2000b) 'Modeling micro-end-milling operations. Part II: Tool run-out', *International Journal of Machine Tools and Manufacture*, Vol. 40, pp.2175–2192.

Bao, W.Y. and Tansel, I.N. (2000c) 'Modeling micro-end-milling operations. Part III: Influence of tool wear', *International Journal of Machine Tools and Manufacture*, Vol. 40, pp.2193–2211.

de Chiffre, L., Kunzmann, H., Peggs, G.N. and Lucca, D.A. (2003) 'Surfaces in precision engineering, microengineering and nanotechnology', *Annals of the CIRP*, Vol. 52, No. 2, pp.561–577.

Dornfeld, D., Min, S. and Takeuchi, Y. (2006) 'Recent advances in mechanical micromachining', *Annals of the CIRP*, Vol. 55, No. 2, pp.745–768.

Dow, T.A., Miller, E.L. and Garrard, K. (2004) 'Tool force and deflection compensation for small milling tools', *Precision Engineering*, Vol. 28, pp.31–45.

Friedrich, C.R. and Vasile, M.J. (1996) 'Development of the micro-milling process for high-aspect-ratio microstructures', *Journal of Microelectromechanical Systems*, Vol. 5, No. 1, pp.33–38.

Ikawa, N., Shimada, S. and Tanaka, H. (1992) 'Minimum thickness of cut in micromachining', *Nanotechnology*, Vol. 3, No. 1, pp.6–9.

Johnson, G.R. and Cook, W.H. (1983) 'A constitutive model and data for metals subjected to large strains, high strain rates and high temperatures', *Proceedings of the 7th International Symposium on Ballistics*, The Hague, The Netherlands, pp.541–547.

Kim, C.J., Bono, M. and Ni, J. (2002) 'Experimental analysis of chip formation in micro-milling', *Transactions of NAMRI/SME*, Vol. 30, pp.247–254.

Kim, C.J., Mayor, J.R. and Ni, J. (2004) 'A static model of chip formation in microscale milling', *ASME Journal of Manufacturing Science and Engineering*, Vol. 126, pp.710–718.

Lee, K. and Dornfeld, D.A. (2002) 'An experimental study on burr formation in micro milling aluminum and copper', *Transactions of NAMRI/SME*, Vol. xxx, pp.255–262.

Liu, X., DeVor, R.E. and Kapoor, S.G. (2006) 'An analytical model for the prediction of minimum chip thickness in micromachining', *ASME Journal of Manufacturing Science and Engineering*, Vol. 128, pp.474–481.

Lucca, D.A. and Seo, Y.W. (1993) 'Effect of tool edge geometry on energy dissipation in ultra precison machining', *Annals of the CIRP*, Vol. 42, No. 1, pp.83–86.

Madou, M. (1997) *Fundamentals of Microfabrication*, CRC Press, Boca Raton, Florida, USA.

Martellotti, M.E. (1945) 'An analysis of the milling process, part ii – down milling', *Transaction of the ASME*, Vol. 67, pp.233–251.

Masuzawa, T. and Tonshoff, H.K. (1997) 'Three-dimensional micro-machining by machine tools', *Annals of the CIRP*, Vol. 46, No. 2, pp.621–628.

Melkote, S.N. and Endres, W.J. (1998) 'The importance of including the size effect when modeling slot milling', *ASME Journal of Manufacturing Science and Engineering*, Vol. 120, pp.68–75.

Özel, T. and Altan, T. (2000) 'Process simulation using finite element method- prediction of cutting forces, tool stresses and temperatures in high-speed flat end milling process', *International Journal of Machine Tools and Manufacture*, Vol. 40, No. 5, pp.713–738.

Schaller, T., Bohn, L., Mayer, J. and Schubert, K. (1996) 'Microstructure grooves with a width of less than 50 micrometer cut with ground hard metal micro end mills', *Precision Engineering*, Vol. 23, pp.229–235.

Schmidt, J. and Tritschler, H. (2004) 'Micro cutting of steel', *Microsystem Technologies*, Vol. 10, pp.167–174.

Schmidt, J., Spath, D., Elsner, J., Huentrup, V. and Tritschler, H. (2002) 'Requirements of an industrially applicable microcutting process for steel micro-structures', *Microsystem Technologies*, Vol. 8, pp.402–408.

Uhlmann, E. and Schauer, K. (2005) 'Dynamic load and strain analysis for the optimization of micro end mills', *Annals of the CIRP*, Vol. 54, No. 1, pp.75–78.

Vasile, M.J., Friedrich, C.R., Kikkeri, B. and McElhannon, R. (1999) 'Micrometer-scale machining: tool fabrication and initial results', *Precision Engineering*, Vol. 19, pp.180–186.

Vogler, M.P., Liu, X., Kapoor, S.G., Devor, R.E. and Ehmann, K.F. (2002) *Development of Meso-Scale Machine Tool (Mmt) Systems*, Technical Paper, Society of Manufacturing Engineers, MS02-181.

Vogler, M.P., DeVor, R.E. and Kapoor, S.G. (2004a) 'On the modeling and analysis of machining performance in micro-endmilling, Part I: Surface generation', *ASME Journal of Manufacturing Science and Engineering*, Vol. 126, pp.685–694.

Vogler, M.P., DeVor, R.E. and Kapoor, S.G. (2004b) 'On the modeling and analysis of machining performance in micro-endmilling, Part II: Cutting force prediction', *ASME Journal of Manufacturing Science and Engineering*, Vol. 126, pp.695–705.

Weule, H., Huntrup, V. and Tritschle, H. (2001) 'Micro-cutting of steel to meet new requirements in miniaturization', *Annals of the CIRP*, Vol. 50, No. 1, pp.61–64.